The SCOPE Dynamic Model for Emulsion Polymerization II. Comparison with Experiment and Applications

EUGENE P. DOUGHERTY, *Research Laboratories, Rohm and Haas Company, P.O. Box 219, Bristol, Pennsylvania 19007*

Synopsis

Paper I provides the underlying theoretical framework for the SCOPE dynamic model of emulsion copolymerization. The present paper compares the model predictions for styrene-methyl methacrylate copolymerizations with experimental measurements made at a variety of polymerization conditions. The SCOPE model predicts conversion–time profiles reasonably well over wide ranges of initiator concentration, monomer concentration and monomer composition. In addition, the model accurately predicts number average molecular weights and copolymer compositions over the entire range of monomer composition. Like previous investigations of this system, the present study suggests that free radical desorption from polymer particles plays a dominant role on the copolymerization kinetics: Simple case II Smith-Ewart kinetics do not apply. The model for this system was applied to understand how changing reaction conditions could effect polymer properties such as particle size and molecular weight distributions. The power of the SCOPE model is illustrated by using it to predict conversion profiles, temperature profiles and copolymer properties for some large-scale versions of these recipes.

I. INTRODUCTION

Paper I[1] presents the theoretical equations used in the SCOPE model. The present paper demonstrates the validity of this computer-based model by comparing predictions made by the model with experimental results for styrene-methyl methacrylate (MMA) emulsion copolymerizations.

Styrene-MMA copolymerization has been investigated extensively by several researchers. Many comparisons made in this study are with experimental results taken (by permission) from Nomura et al.,[2] who recently made a comprehensive kinetic study of styrene-MMA emulsion copolymerizations. Over 20 batch emulsion copolymerization experiments were run at many different conditions. These experiments examined the effects of initiator concentration, starting monomer composition, particle size, particle concentration, and monomer concentration on the conversion-time profiles. The slope of the conversion-time profile yielded an overal polymerization rate. Nomura et al. constructed a kinetic model to interpret the results. They concluded that the system did not observe Smith-Ewart case II kinetics, as one might expect, but instead that radical desorption played a significant role.

This report shows how the experiments reported in Ref. 2 and elsewhere confirm the validity of the SCOPE model as a useful tool to understand emulsion copolymerization. Also, this report applies the model to comple-

Journal of Applied Polymer Science, Vol. 32, 3079–3095 (1986)
 CCC 0021-8995/86/013097-17$04.00

ment and extend the experimental results. Section II of this paper provides computational details pertinent to the calculations. A detailed comparison of model predictions with experimental results for Styrene-MMA copolymerizations is provided in Section III. Section IV applies SCOPE to determine how process modifications influence the polymerization rate, copolymer composition, molecular weight, and particle size development. Perhaps the most useful application of the SCOPE model is provided in Section V, where the model is applied to evaluate three different scenarios for production-sized versions of one of the recipes from Ref. 2. Some future directions for understanding and controlling emulsion polymerization processes are suggested in Section VI.

II. COMPUTATIONAL DETAILS

In order to compare SCOPE model predictions with available experimental results, 20 computer simulations were run. With enough parameters, any of a variety of models can fit experimental data very precisely for a single set of conditions. A reliable model is sufficiently robust to predict trends accurately when conditions are varied substantially. Therefore, SCOPE was tested on a system where conditions span wide ranges of particle size, initiator level, monomer concentration, and monomer composition (Table I).

The first 16 runs were made to compare with the conversion-time profiles of Ref. 2, while the last four were made to compare with properties reported in Ref. 3. In general, the simulations were run exactly as the experiments were described in the literature: runs 1 through 16 were seeded batch

TABLE I
Initial Conditions Used for the Styrene/MMA Calculations

Run number	Particle size (nm)	Particles per cc H_2O	KPS conc. (g/L H_2O)	Monomer conc. (g/cc H_2O)	Monomer comp. (Sty/MMA)
1	55	1.50E+14	1.25	0.097	95/5
2	55	1.50E+14	1.25	0.097	25/75
3	55	1.50E+14	1.25	0.097	50/50
4	55	1.50E+14	0.13	0.097	50/50
5	55	1.50E+14	0.50	0.097	50/50
6	55	1.50E+14	2.50	0.097	50/50
7	40	1.00E+14	1.25	0.099	50/50
8	40	1.00E+14	1.25	0.050	50/50
9	40	1.00E+14	1.25	0.197	50/50
10	40	1.00E+14	1.25	0.299	50/50
11	40	5.00E+13	1.25	0.100	50/50
12	40	4.00E+14	1.25	0.097	50/50
13	55	5.00E+13	1.25	0.025	50/50
14	55	1.00E+14	1.25	0.050	50/50
15	55	2.00E+14	1.25	0.100	50/50
16	55	4.00E+14	1.25	0.200	50/50
17	—	0.0	5.55	0.555	24.2/75.8
18	—	0.0	5.55	0.555	39.1/60.9
19	—	0.0	5.55	0.555	54.0/46.0
20	—	0.0	5.55	0.555	69.2/30.8

copolymerizations, using soap levels sufficiently low to prohibit particle generation; runs 17 through 20 were unseeded batch copolymerizations, which used the recipe described in Ref. 3.

All calculations reported in this paper used the parameters listed in Table II. Some of these parameters were taken directly from the literature. Some parameter estimates had to be refined to fit the experimental data. The literature values for k_p and k_t, for example, were modified to give the correct behavior in the high-conversion (diffusion-controlled) regime. Also, experimental data from Ref. 2 was used to determine a value for the radical desorption rate constant, k'_{de}. As stated above, radical desorption is believed to play a dominant role in determining the average number of radicals per particle in styrene-MMA emulsion copolymerizations.[2]

Physical property information, that is, densities, molecular weights, and heat capacities, were obtained from Refs. 6 and 9.

TABLE II
Kinetic Parameters Used in the Styrene/MMA Calculations

Parameter	Value	Units	References
f_o	0.76[a]	—	3,4
k_d	6.2E16 exp(−33500/RT)	sec^{-1}	5
k_{p11} (Styrene)	$\frac{8.6E7}{1 + 8x^{12}}$ exp (−8100/RT)	$\frac{\text{liters}}{\text{mole sec}}$	6
k_{p22} (MMA)	2.5 k_{p11}	$\frac{\text{liters}}{\text{mole/sec}}$	2,3,6
k_{td}	$\frac{2.0E11}{1 + 140x^4}$ exp (−7650/RT)	$\frac{\text{liters}}{\text{mole sec}}$	6
k_{tc}	0.01 k_{td}	$\frac{\text{liters}}{\text{mole/sec}}$	—
k'_{de}	1.35E11	$\frac{\text{liters}^{2/3}}{\text{mole/sec}}$	—
$k_{\text{tr-Styrene}}$	4.5E-4 $\bar{k}_p$	$\frac{\text{liters}}{\text{mole/sec}}$	2,3,7,8
$k_{\text{tr-MMA}}$	1.5E-5 $\bar{k}_p$	$\frac{\text{liters}}{\text{mole/sec}}$	2,3,7,8
a_1	0.18	—	—
a_2	1.00[b]	—	—
$\bar{x}_c$	0.38	—	2,3
r_{12}	0.52	—	2,3,6
r_{21}	0.46	—	2,3,6
a_s	41.5	$\frac{\text{Angstroms}^2}{\text{molecule}}$	3
$(S)_{\text{cmc}}$	0.0120	mole/liter	—
q	2.7	—	—
μ	0.0	$\text{liter}^{-1/3}$	—
γ	3.5	—	—
d_m	75.0	Angstroms	—

[a] The reference initiator concentration, $[I_o]$, is 1.25 g/L water.

[b] At lower monomer concentrations, a greater fraction of monomer is soluble in the aqueous phase; therefore $a_2 = 0.66$ at 0.025 g monomer per cc water, $a_2 = 0.83$ at 0.05 g monomer per cc water.

III. COMPARISON WITH EXPERIMENT

Figures 1–5 compare calculated and observed conversion-time profiles. Gravimetric methods were used in Ref. 2 to determine the experimentally observed conversions. Since no replication was done, it is difficult to estimate the experimental error. Overall, agreement between the SCOPE calculations and the experimentally observed conversion rates is quite good. More important, the model predicts every qualitative trend indicated by the experiments. The average root-mean-square deviation between model and experiment is 7.43% (conversion), much of the deviation being contributed by only three of the sixteen runs.

Figure 1 assesses the effect of initiator concentation on the conversion rate. The agreement of model and experiment is remarkably good, even though the initiator concentration changes by a factor of 50. Naturally, increasing the initiator concentration markedly increases the conversion rate. Moreover, for the highest two initiator concentrations (1.25 and 2.50 g potassium persulfate per liter of water), an accelerated conversion rate is observed around 50% conversion. The accelerated rate indicates that the termination rate is becoming more diffusion controlled.[10,11] At still higher conversions (> 90%) the propagation rate becomes diffusion controlled, for the polymerization levels off at conversions less than 100%. SCOPE accounts for both phenomena, although some lack of fit is observed. The observed lack of fit is probably due to poor parameter estimates, but experimental difficulties involved in sampling a rapidly polymerizing emulsion may be playing some role.

Figure 1 shows that the persulfate initiator is less effective at increasing the polymerization rate at higher concentrations. As we noted in paper I,

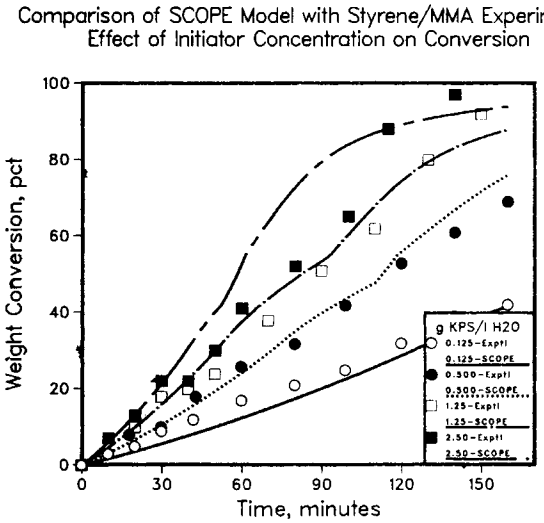

Fig. 1. Conversion rate versus time for various starting initiator concentrations. In Figures 1–5, the lines indicate results of SCOPE simulations; plotting symbols refer to corresponding experimental results reported in Ref. 2. Solid line and open circles refer to 0.125 g potassium persulfate (KPS) per liter of water; dotted line and bullets, 0.500 g KPS/L H_2O; open squares and dashed-dotted line, 1.25 g KPS/L H_2O; and darkened squares and dashed line, 2.50 g KPS/L H_2O.

this decreased efficiency at higher initiator concentrations has previously been observed by Blackley[12] Hakoila.[13]

The effect of starting monomer concentration is presented in Figure 2. Intuitively, one might expect the conversion rate to be about the same at the higher concentrations, since the rate of propagation is proportional to the monomer concentration in the particles. Interestingly, while the polymerization rate is faster, the overall conversion rate drops at higher monomer concentrations. This is mainly because the polymer particles get saturated with monomer. With more monomer to convert, the particles stay saturated with monomer for a longer time, the gel effect is delayed, and the conversion rate is slower than expected. SCOPE predictions over the range investigated by Nomura et al.[2] were reliable and quantitative. The observed lack of fit at longer times for the lowest conversions is probably due to inexact estimates of the diffusion-controlled termination rate.

Figure 3 assesses the effect of monomer composition on conversion rate. While the agreement is generally good, the model underestimates the conversion rate for the 95% Styrene/5% MMA starting composition. Undoubtedly, this lack of fit is partly due to assuming a single termination rate to apply over the entire composition range. Technically there are three termination rate constants: styryl radicals terminating with each other, MMA radicals with each other, and cross-termination of styryl and MMA radicals. These rate constants will differ, since the styryl radical is resonance stabilized to a greater degree than the MMA radical. Moreover, MMA has a more pronounced autoacceleration effect than does styrene. Hamielec and MacGregor[14] have suggested that initiator efficiency may be affected by copolymer composition. Despite these complications, the model and experiment agree very well over a wide compositional range. Different equations

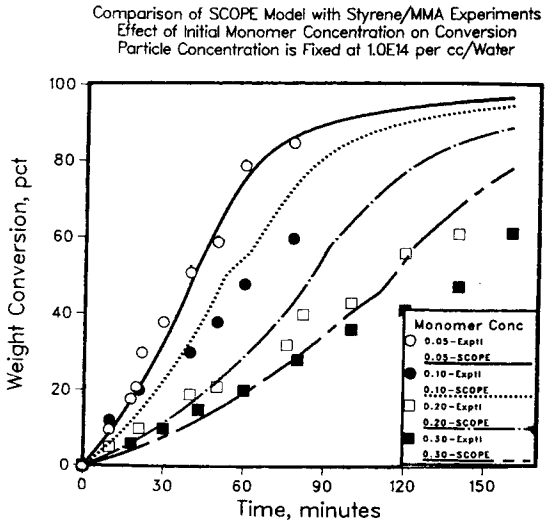

Fig. 2. Conversion rate versus time for various initial monomer concentrations at a fixed particle concentration. (See also caption for Figure 1.) Solid line and open circles refer to a starting monomer weight fraction of 0.05; dotted line and bullets, 0.10; open squares and dashed-dotted line, 0.20; and darkened squares and dashed line, 0.30.

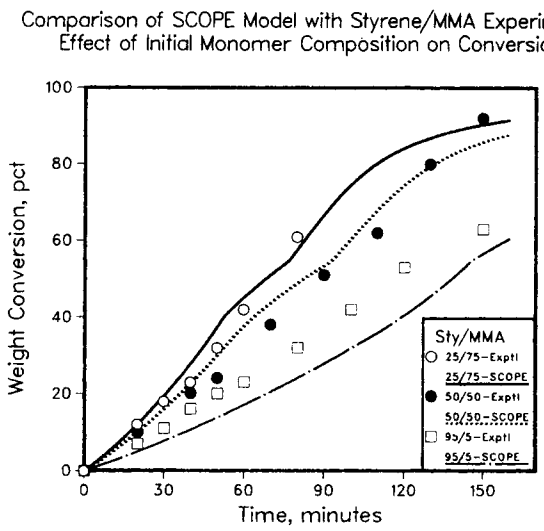

Fig. 3. Conversion rate versus time for various initial monomer compositions. (See also caption for Figure 1.) Solid line and open circles refer to a starting composition of 25% Styrene, 75% MMA; dotted line and bullets, 50% Styrene, 50% MMA; open squares and dashed-dotted line, 95% Styrene, 5% MMA.

and more precise parameter estimates would be required to obtain perfectly quantitative results. In any event, the "inhibiting" effect that styrene usually exhibits in copolymerizations with acrylic monomers is clearly indicated by both the SCOPE model and the experiments.

Figure 4 determines the effect of particle concentration on conversion

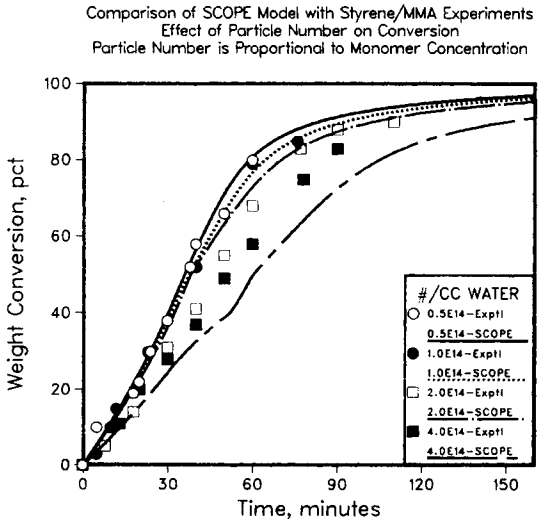

Fig. 4. Conversion rate versus time for various initial concentrations of polymer particles. Here the particle number is in direct proportion to the starting monomer concentration. (See also caption for Figure 1.) Solid line and open circles refer to a starting concentration of 0.5E14 particles per liter of water; dotted line and bullets, 1.0E14 particles per L H_2O; open squares and dashed-dotted line, 2.0E14 particles per L H_2O; darkened squares and dashed line, 4.0E14 particles per L H_2O.

rate. In these experiments the starting monomer concentration was purposely chosen to be proportional to the particle concentration. The SCOPE model observes the experimental trend that increasing both particle concentrations and monomer concentrations together decreases the conversion rate only slightly. For runs 13 and 14 particle concentrations and monomer concentrations were very low. Reference 2 pointed out that at such low monomer concentrations an appreciable portion of MMA monomer would be soluble in the aqueous phase rather than in the polymer phase. Thus, the partitioning coefficient, a_2, was taken to be 0.66 for run 13 and 0.83 for run 14. This gave excellent agreement with experimental results. The underlying theory for how monomers partition themselves among the aqueous phase, the monomer droplets, and the polymer particles is rather involved. Uglestad[15] has made significant progress in understanding the thermodynamics of swelling of polymer particles by several components over a range of particle sizes. Moreover, the UNIFAC approach[16,17] appears to be promising for calculating the partitioning of components in the various phases. Fitzwater[18] has made some progress in adapting UNIFAC to deal with emulsion copolymer systems. Still, much work needs to be done to obtain reliable, quantitative results. As the theory develops and as parameters become better known, model predictions will improve.

Figure 5 determines the effect of particle concentration on conversion rate at a fixed monomer concentration. As expected, an increased rate at higher particle concentrations is observed; the SCOPE model follows this trend. However, while the agreement of model and experiment is good for the first 40 minutes or so, afterwards the model exhibits lack of fit, underestimating the effect of the increased particle concentration on conversion rate. On the other hand, simple case II Smith-Ewart kinetics overestimates the effect of particle concentration. Interestingly, the kinetic model devel-

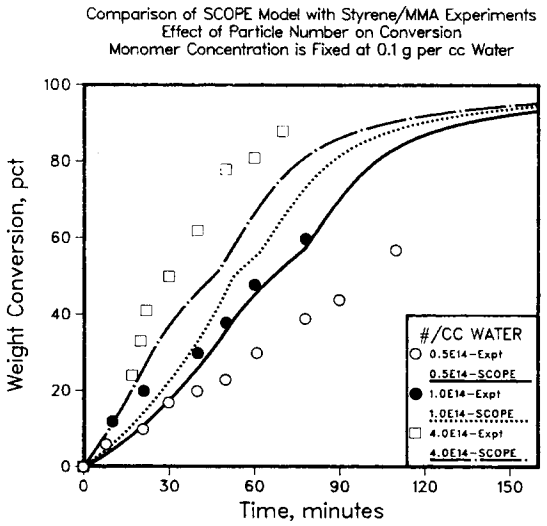

Fig. 5. Conversion rate versus time for various initial particle concentrations at a fixed monomer concentration. (See also caption for Figure 1.) Solid line and open circles refer to a starting concentration of 0.5E14 particles per liter of water; dotted line and bullets, 1.0E14 particles per L H_2O; open squares and dashed-dotted line, 4.0E14 particles per L H_2O.

oped by Nomura et al.[19] to calculate the copolymerization rate at 35% conversion also underestimated the effect of particle concentration at all monomer concentrations studied.

Because both the SCOPE model and Nomura's model underestimate the particle concentration effect while Smith-Ewart case II kinetics overestimates the effect, the number of radicals per particle is a more complicated function of particle size and composition than expected. The SCOPE model includes initiation, propagation, termination, and desorption reactions; however, lack of fit is still observed in Figure 5. Trace impurities can exert substantial effects.[14] Particle morphology may play some role: slow intraparticle diffusion may result in a core-shell morphology which could complicate the kinetics.[20] Nomura et al.[19] also had trouble fitting this data using a slightly different kinetic model. More careful nonlinear parameter estimation procedures would certainly give better agreement with experiment. In particular, the radical desorption rate constant and its correlation with particle size should be reexamined.

While SCOPE predicts conversion-time profiles reasonably well, it also predicts many other properties important for polymer quality: molecular weight distribution, particle size distribution, and copolymer composition, and so on. These properties are often difficult and expensive to measure, so being able to predict their trends over time can be quite useful.

Some measurements of polymer quality—copolymer composition and molecular weight as a function of styrene starting composition—were reported in Ref. 3 for batch styrene-MMA emulsion copolymerizations. Simulations 17 through 20 wewre run to compare with the reported results. As Table III indicates, SCOPE predicts copolymer compositions and number average molecular weights quite accurately over a wide range of starting styrene compositions. In light of Figure 3, the agreement of computed and observed copolymer compositions is as expected. Since the conversion-time profiles agree over a wide range of starting styrene compositions, the copolymer compositions should agree as well. The number average molecular weights predicted by the model simulations are also consistent with an earlier result reported by Gardon[21] for the number average molecular weight of MMA homopolymer (4.11E6) as well as other results previously reported in the literature.[7,8,21,22]

In summary, the SCOPE model qualitatively predicts every major trend noted in the experiments. It reliably predicts the conversion at any time to within 15 wt % over a wide range of initiator concentrations, monomer

TABLE III
Comparison of SCOPE Model Predications with Experimental Results (Ref. 3) for Copolymer Composition and Molecular Weight

Mole fraction of styrene in the monomer mix	Mole fraction of styrene in the copolymer		Number average molecular weight (x1.0E6)	
	SCOPE	Experimental	SCOPE	Experimental
0.242	0.317	0.329	3.16	3.56
0.391	0.434	0.430	2.71	2.90
0.540	0.536	0.498	2.29	2.31
0.692	0.625	0.619	1.93	2.10

concentrations, particle concentrations, and monomer compositions. Moreover, the copolymer compositions and number average molecular weights computed by SCOPE agree with the available experimental results to within 10 percent. Much of the lack of fit observed in the conversion-time profiles is due to poor parameter estimates. Well-designed experiments and accurate nonlinear estimation procedures would yield better results. Still greater accuracy could be achieved from a more fundamental understanding of the following phenomena: diffusion-controlled reactions, partitioning of monomer in the aqueous and organic phases, and the interrelationships among the average number of radicals per particle, the particle size, and particle composition.

IV. APPLICATION OF THE SCOPE MODEL TO UNDERSTAND PROCESS DYNAMICS

SCOPE can be applied to extend our knowledge of Styrene-MMA copolymerizations by predicting trends in conversion-time profiles, molecular weights, and copolymer compositions without direct experimental measurements. For instance, results of simulations listed in Table I can be used to understand how changing the initiator, monomer, and particle concentrations affects polymer properties. To illustrate, Figure 6 provides plots of time versus particle size, molecular weight, instantaneous copolymer composition, and overall polymerization rate at the four initiator concentrations investigated in Ref. 2. The plots were purposely made on the same figure to show how the profiles relate to each other.

While the conversion rates shown in Figure 1 are well behaved, the copolymerization rate profiles predicted by SCOPE (Fig. 6) exhibit more complex structure. At the lowest initiator level (0.125 g/L water) the rate is almost constant and quite slow. At higher concentrations the copolymerization rate increases as the termination rate becomes more diffusion controlled. After peaking, the rate drops as the monomer concentration in the particles drops from the saturation concentration. The propagation rate, which becomes diffusion controlled at high (ca. 95%) conversion, causes the conversion rate to drop to nearly zero.

Average particle diameters follow the copolymerization rate. The monomer swells seed particles (seed diameter = 55 nm) very rapidly at the start of the process to about 80 nm. The increase in particle size continues more gradually as the polymerization proceeds. The particles continue increasing in size until the monomer droplets disappear at the critical conversion (40%), at which point they begin to shrink. At this conversion, particles become less rich in monomer, which occupies a greater specific volume than the copolymer. The lowest initiator concentration run never reaches 40% conversion, so no maximum peak diameter is reached. Curiously, the run at the highest initiator concentration exhibits two peaks. After the droplets disappear, the rate continues to accelerate, causing the occurrence of a second peak before leveling off to the final particle size of 130 nm.

The instantaneous copolymer composition does not differ much from the 50/50 composition used in all four runs. At the beginning of the copolymerization, the instantaneous copolymer composition is only slightly richer in styrene. Only at the end of the copolymerization does the instantaneous

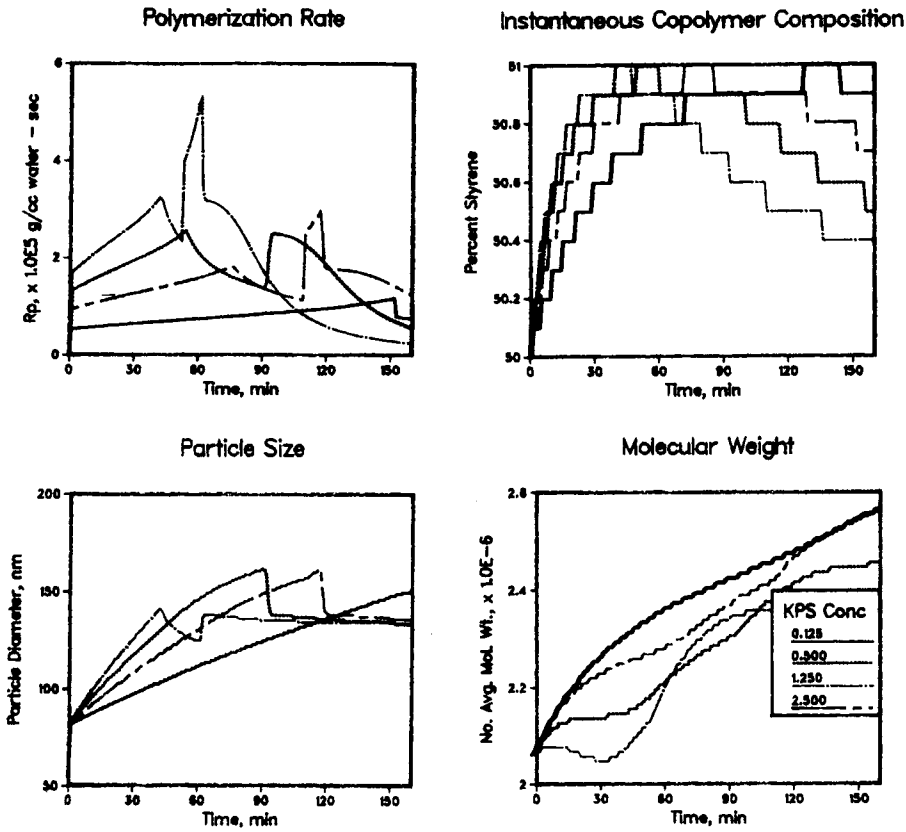

Fig. 6. Results of simulations using the SCOPE model at selected initiator concentrations. Results are displayed over the same time scale for polymerization rate, instantaneous copolymer composition, particle size, and molecular weight. Recipes given in Table I were used in the calculations. The solid line refers to 0.125 g potassium persulfate (KPS) per liter of water; dotted line, 0.500 g KPS/L H_2O; dashed-dotted line, 1.25 g KPS/L H_2O; and dashed line, 2.50 g KPS/L H_2O.

copolymer composition become MMA rich. This is because the slightly less reactive MMA accumulates in the residual monomer mixture. Ironically, styrene converts slightly more rapidly than MMA, while styrene exerts an inhibiting effect overall in copolymerization with acrylic monomers (see Fig. 3). The resonance stability of the styryl radical causes this inhibiting effect.

The predicted molecular weight profiles for these runs are particularly intriguing. As stated above, number average molecular weight predictions made by SCOPE exhibit good agreement with the results of several experimental investigations.[3,7,8,21,22] These experimental studies indicate that transfer-to-monomer largely controls the molecular weight. Test calculations carried out using different transfer-to-monomer rate constants indicated this to be the case.

As Figure 6 indicates, the polymerization runs made at the lowest and highest initiator concentrations produced the highest molecular weight polymer (about 2.75 million at 160 min). Curiously, runs made at inter-

mediate concentrations produced lower molecular weight polymer. In fact, at 1.25 g/L, the molecular weight first increases, then drops to a minimum around 30 min into the reaction and finally increases again before leveling off around 2.35 million or so. The variations in molecular weight with polymerization time in a batch reactor are noteworthy. While such differences would likely not seriously affect polymer performance, they do illustrate that simple statements like "increasing the initiator concentration decreases molecular weight" can be misleading and often erroneous. The subtle interplay of propagation, termination and transfer reactions can often produce complicated molecular weight profiles.

V. APPLICATION OF SCOPE TO EVALUATE PROCESSING CONDITIONS FOR SCALE-UP

Through computer simulations and graphics, one can rapidly screen a large number of potential processing conditions to decide which would be most promising to try out in the pilot plant. Accurate computer simulations and a few pilot plant runs would necessitate only a minimum number of expensive and perhaps unsafe experiments in production-sized reactors. From simulations one can determine how temperature profiles change as a particular recipe is scaled up from lab to pilot plant to production-size reactors. Equipment can be appropriately sized, effects of efficient and poor heat transfer can be properly assessed, and in-plant controllers can be tuned using computer simulations as a guide.

This section of the paper applies SCOPE to evaluate three sets of processing conditions which might conveivably be used to scale up one of the runs from Ref. 2. Unlike the batch experiments of Ref. 2, however, the three runs made here are seeded, semibatch copolymerizations. Table IV lists processing conditions and equipment parameters used in the three simulations. These conditions and parameters are roughly comparable to those which might be used for small-scale production. Once again, Table II lists the kinetic parameters. Table IV lists the conditions for the "base case" simulation. Two other simulations were run using almost the same parameters as for the "base case." The set point was increased from 55 to 60°C in the second simulation. In the third, the initiator concentrations were doubled.

Figures 7 through 10 summarize the results of the simulations graphically. Figure 7 provides plots of weight conversion, reactor temperature, coolant temperature and the (manipulated) monomer emulsion flow rate. As Figure 7 shows, addition of cool monomer (inlet temperature = 45°C) causes the reactor temperature to drop during the first hour from the starting temperature of 55°C. The decreasing temperature and the PI control algorithm used increase the monomer emulsion feed rate. The maximum allowable flow rate of 64 lb/min is reached after about an hour. During the second hour the increased flow rate causes the reactor and coolant temperatures to increase, which in turn causes an increased conversion rate. Around 50% conversion the copolymerization begins to autoaccelerate: dramatic increases in temperature and conversion are observed. In the third hour the PI control algorithm causes the monomer emulsion flow rate to decrease to zero.

TABLE IV
Processing Conditions and Recipe for the Three Scale-up Runs

Reactor diameter	6.0	ft	
Reactor height	9.0	ft	
Cooling water jacket thickness	0.5	in	
Cooling water flow rate	8.0	gal/min[a]	
Starting monomer emulsion flow rate	12.7	lbs/min	
Maximum monomer emulsion flow rate	64	lbs/min	
Set-point temperature	55	°C[b]	
Starting reactor temperature	55	°C	
Starting coolant temperature	45	°C	
Inlet emulsion feed temperature	45	°C	
Inlet coolant temperature	45	°C	
Emulsion controller starts	10	min after feed starts	
Proportional band for emulsion controller	−0.2	pct	
Integral constant for emulsion controller	0.006	pct/sec	
Derivative constant for emulsion controller	0.0	sec/pct	
Time constant for temperature measurement	1.0	min	
Heat transfer coefficient	48.0	Btu/(ft²-hr-°F)	
Water	65.8		6582.1
Polymer seed (55 nm, $\overline{M}_N$ = 2.0E6	14.2		0.0
Styrene	0.0		658.2
Methyl methacrylate	0.0		658.2
Initiator (KPS)	0.823[c]		8.23[c]
Soap	10.0		15.0

[a] For the first 11 minutes, the cooling water flow rate was only 1.6 gal/min.

[b] This quantity was changed to 60°C for the simulation labelled "SET.PT.=60" on Figs. 7 and 8.

[c] These quantities were doubled for the simulation labelled "KPS × 2" in Figs. 7 and 8.

Clearly, Figure 7 shows that the run at the higher initiator concentrations exhibits much different process dynamics than those for the other two simulations. The conversion rate is higher from the start of the process; thus the temperature remains above 47°C for the entire process. Since the temperature is closer to the set-point, the PI controller increases the monomer emulsion flow rate less rapidly for this ran than for the other two runs. With the present control procedure and parameters, SCOPE predicts the initiator-rich run to give the best process control fo the three runs. The other two runs increased the monomer emulsion flow rate so quickly that the temperature increased sharply during the third hour. The result was that the flow rate then had to be sharply decreased, and thus, the process feed could not be added within four hours for these two runs. On the other hand, for the initiator-rich run, the entire process feed was added within four hours; moreover, temperature control was better.

The high initiator concentration run exhibits not only different process dynamics but different copolymer properties as well. Not surprisingly, Figure 8 shows that the initiator-rich run exhibits a faster copolymerization rate. This, in turn, causes the instantaneous copolymer composition to be initially richer in styrene, then later richer in MMA. This occurred in the other two runs as well, but at much later process times. Thus, the microstructure of the copolymer chains would differ slightly for this run.

Interestingly, all three simulations exhibit oscillatory copolymerization

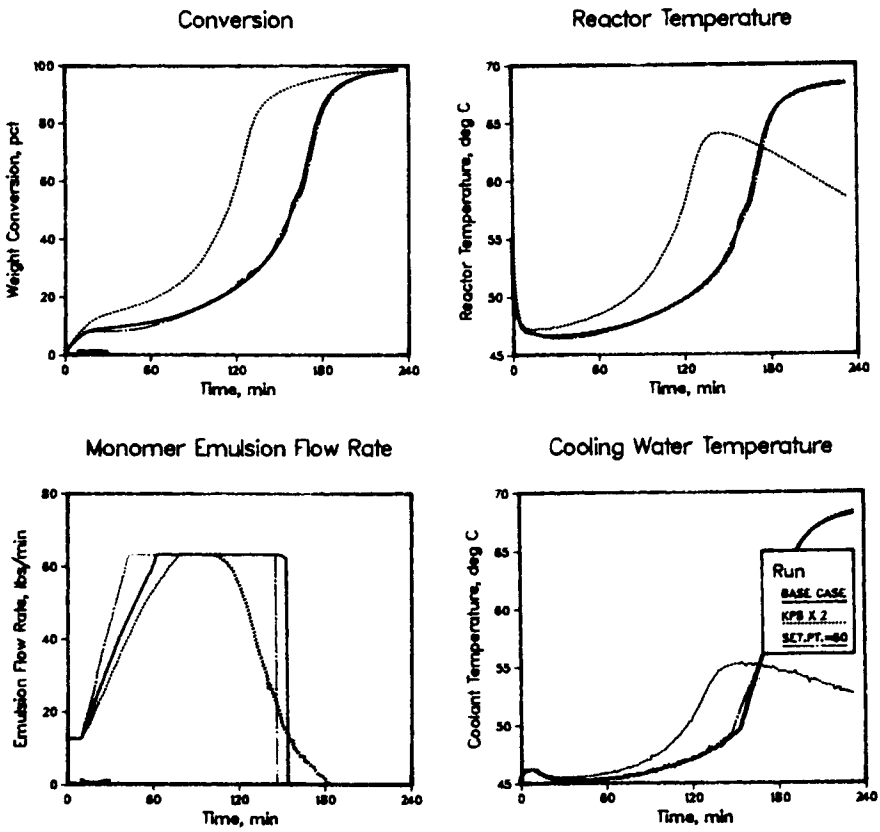

Fig. 7. results of simulations using the SCOPE model for the various scale-up scenarios described in Table IV. The solid line indicates results for the base case calculation, the dotted line, for calculations where the initiator concentration was doubled over that of the base case, and the dashed-dotted line gives results for a higher temperature set point (60 rather than 55°C).

rates, particularly near the onset of the rapid temperature rise. These oscillations result from the competition of three mechanisms: the rate of monomer addition, which serves to increase the rate by adding fresh monomer to the system; the decrease in monomer concentration in the particles as the droplets disappear; and the termination rate, which becomes increasingly diffusion controlled.

Particle-size profiles for these semibatch runs result from the competing effects of particle nucleation and particle growth. Soap concentrations are high enough to generate new particles during the first half-hour of the process. On the other hand, growth of polymer particles present initially (seed diameter = 55 nm) competes with particle nucleation. Figure 9 shows how particle nucleation and growth can change how the particle-size distributions evolve over time. Twenty minutes after the feed begins, almost all particles have diameters in the 90 nm range, which is approximately the diameter of the seed particles swollen with monomer. By 40 minutes, practically 55% of the particles have diameters < 20 nm; thus, a large number of particles have been nucleated early in the process. Afterwards,

these particles grow out as two separate populations, resulting in a particle size distribution exhibiting two distinct peaks. Actually, while the number percentage of particles in the small mode is high, the weight percentage of small-mode particles is too low to influence the average particle diameters: no drop in particle diameter is observed in the first half-hour due to nucleation (see Fig. 8).

The particle diameter profiles for the initiator-rich run differ slightly from those for the other two runs. Initially, the diameters are a little lower, presumably because the higher radical flux produces new (smaller) particles more rapidly. As the rate of copolymerization increases, the particles grow more rapidly for the initiator-rich runs. A momentary decrease in size occurs when the monomer droplets disappear around 120 min for the initiator-rich run and at 180 min for the other two runs. The final particle diameter is lowest for the initiator-rich run, becuase a greater number of small-mode particles are produced at the higher radical concentrations.

Molecular weight profiles, too, are different for the initiator-rich run. The somewhat complicated effect of initiator concentration on molecular weight observed for the batch runs (see Fig. 6) is observed for these semibatch runs as well. Increasing the initiator concentration seems to decrease the molecular weight, although the increase in copolymerization rate caused by higher initiator concentrations is a mitigating factor.

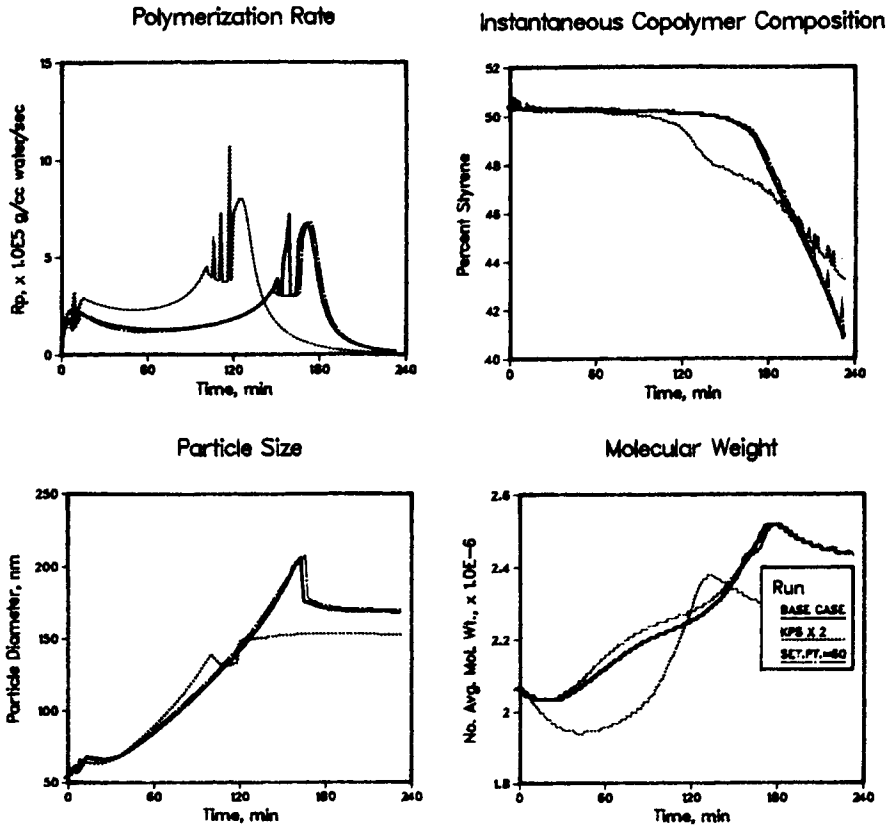

Fig. 8. Additional SCOPE simulation results. (See caption for Figure 7.)

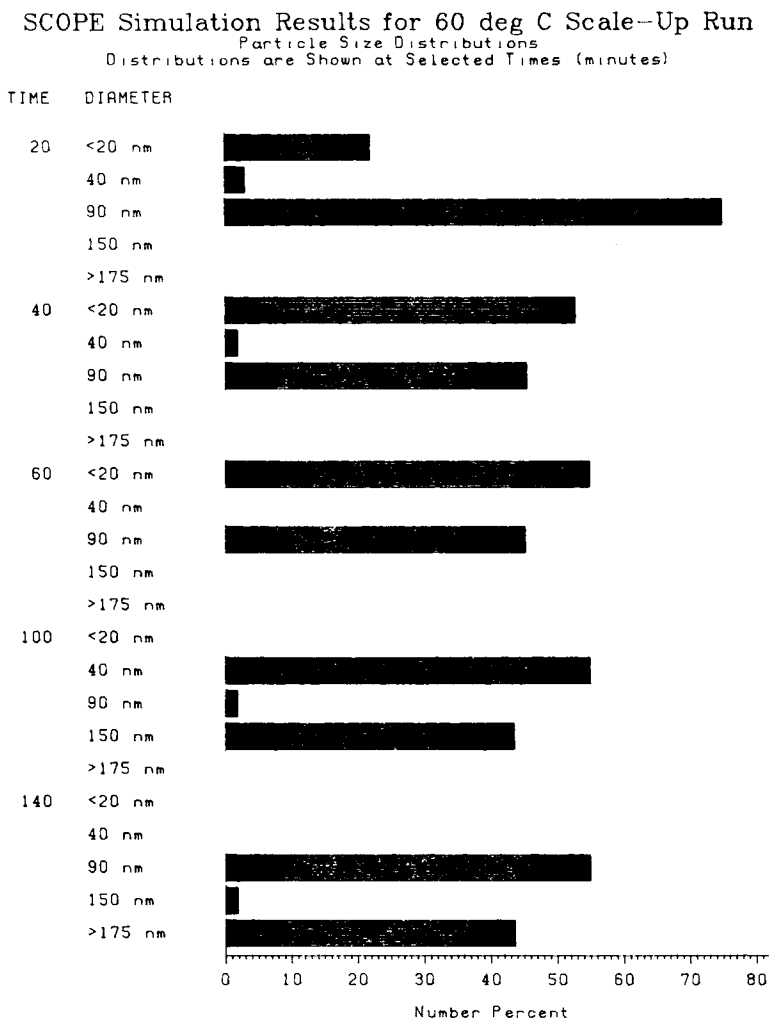

Fig. 9. Particle size distributions at selected times calculated using the SCOPE model for the recipe given in Table IV. (Set point temperature = 60°C).

Figure 10 shows how the cumulative molecular weight distributions change with time for the 60°C set-point simulation. At 20 min, the cumulative molecular weight distribution is narrow and centered about a large peak at 2 million. At 120 min the cumulative distribution broadens and shifts toward higher molecular weights, mainly because the propagation rate is becoming faster relative to termination. At 220 min the cumulative number average molecular weight distribution is broader yet, with a substantial fraction having a molecular weight exceeding 4 million. By 220 min the number average molecular weight increases to about 2.3 million, while the polydispersity increases from about 2 at 20 min to about 3 at 220 min. Molecular weight distributions reflect the complex, wide-ranging kinetic and process behavior characteristic of controlled, semibatch copolymerization processes.

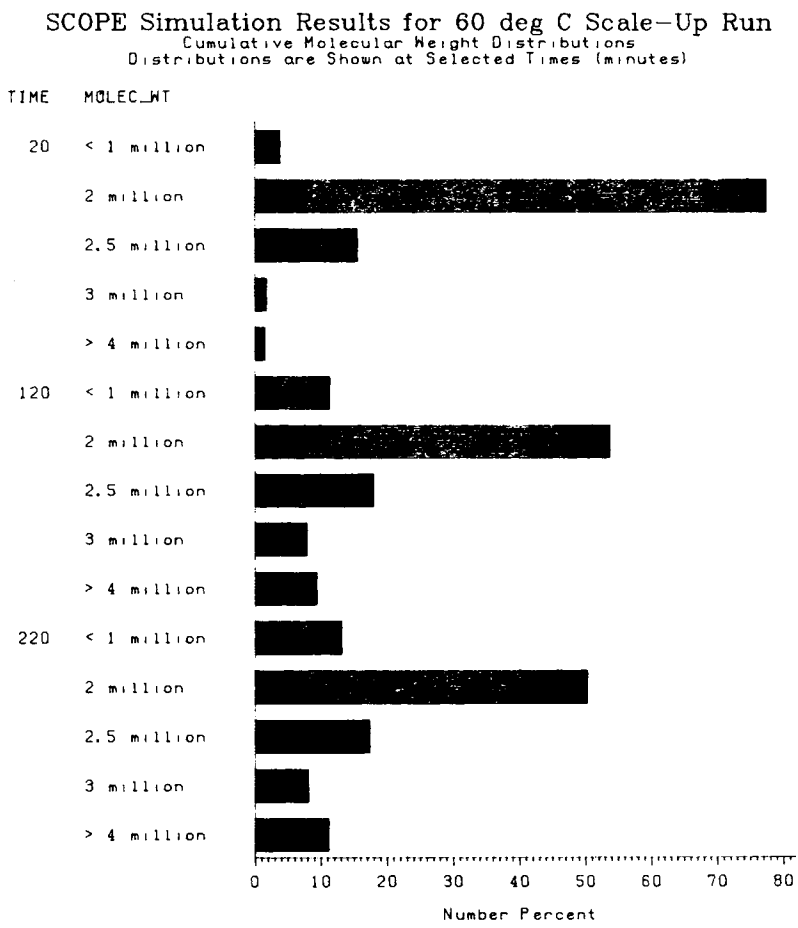

Fig. 10. Molecular weight distributions at selected times calculated using the SCOPE model for the recipe given in Table IV. (Set point temperature = 60°C).

VI. CONCLUDING REMARKS

The SCOPE model correctly predicts the effects of a number of process variables in styrene-MMA copolymerizations and can give insight into the interrelationships among variables for large-scale recipes for which experiments are difficult and expensive to perform.

While the SCOPE model can determine the effects of processing conditions on the complex process of emulsion copolymerization, it still cannot predict with complete quantitative accuracy. As stated above, SCOPE slightly underestimates the effects of particle concentration on conversion rate at fixed monomer concentrations. To be sure, refinements are necessary and fundamental work needs to be done in the following areas: determination of molecular weight when chain-branching reactions are important; diffusion-controlled reactions in small emulsion particles; particle nucleation; particle morphology; and partitioning of monomer in aqueous, polymer, and droplet phases.

The SCOPE model can be used in conjunction with on-line process measurements for better process control. Using techniques like time series analysis[23] and Kalman filtering,[24] data can be used to refine model predictions so that emulsion polymerization processes can be better understood and more accurately controlled.

The author would like to thank the Rohm and Haas Company, in particular, Dr. Robert Naylor, for granting permission to publish this work. He also gratefully acknowledges Prof. M. Nomura, who supplied detailed experimental information to this study; Mrs. Elizabeth Broodno, who assisted with the preparation of this manuscript and the graphics; and Dr. Kayson Nyi and Mr. James Holahan, who made useful suggestions on the manuscript.

References

1. E. P. Dougherty, *J. Appl. Polym. Sci.*, **29**, (1986).
2. M. Nomura, K. Yamamoto, I. Horie, K. Fujita, and M. Harada, *J. Appl. Polym. Sci.*, **27**, 2483 (1982).
3. J. M. Goldwasser and A. Rudin, *J. Polym. Sci. Polym. Chem. Ed.*, **20**, 1993 (1982).
4. A. Rudin, M. C. Samanta, and B. M. E. Van der Hoff, *J. Polym. Sci. Polym. Ed.*, **17**, 493 (1979).
5. I. M. Kolthoff and I. K. Miller, *J. Am. Chem. Soc.*, **73**, 3055 (1951).
6. J. Brandup and E. H. Immergut, *Polymer Handbook*, Wiley, New York, 1975.
7. M. S. Matheson, E. Auer, E. Bevilacqua, and E. J. Hart, *J. Am. Chem. Soc.*, **71**, 497 (1949).
8. M. Stickler and G. Meyerhoff, *Makromol. Chem.*, **179**, 2714 (1978).
9. Tables of FLOWTRAN Component Physical Properties, Monsanto, St. Louis, Mo., December 1981.
10. S. K. Soh and D. C. Sundberg, *J. Polym. Sci.*, **20**, 1345 (1982).
11. F. L. Marten and A. E. Hamielec, *ACS Symposium Series*, **104**, 43 (1979).
12. D. C. Blackley, *Emulsion Polymerization*, Wiley, New York, 1975.
13. E. Hakoila, *Annales Univeristatis Turkuensis*, Ser. A 66, **7**, (1963).
14. A. E. Hamielec and J. F. MacGregor, Course Notes, "Polymer Reaction Engineering," McMaster University, Hamilton, Ontario, Canada, May 1985.
15. See, for example, J. Uglestad, P. C. Mork, A. Berge, T. Ellingsen, and A. A. Khan, in *Emulsion Polymerization*, ed. I. Piirma, Academic, New York, 1982 pp. 383–413.
16. W. R. Krigbaum and D. K. Carpenter, *J. Polym. Sci.*, **14**, 241 (1954).
17. J. M. Prausnitz and Oisi, IE&C Chem. Proc. Des. Dev., **17**, 330 (1978).
18. S. Fitzwater, to be published.
19. M. Nomura, M. Kubo, and K. Fujita, *J. Appl. Polym. Sci.*, **28**, 2767 (1983).
20. C.-I. Kao, D. I. Lee, and E. F. Stevens, *J. Dispersion Sci. Technol.*, **5**, 283 (1984).
21. J. L. Gardon, *J. Polym. Sci.*, A-1 **6**, 623 (1968).
22. J. L. Gardon, *J. Polym. Sci.*, A-1 **6**, 687 (1968).
23. G. E. P. Box and G. M. Jenkins, *Time Series Analysis, Forecasting and Control*, Holden Day, San Francisco, 1976.
24. See, for example, K. J. Astrom, *Introduction to Stochastic Control Theory*, Academic, New York, 1970; C. Kiparissides, J. F. MacGregor, and A. E. Hamielec, *J. Appl. Polym. Sci.*, **23**, 401 (1979).

Received September 19, 1985
Accepted November 12, 1985